

Inter-System Handover and Coverage Detection for 3G/WLAN Cooperation

- Invited Paper -

Matthias Siebert¹, Daniel Bültmann¹, Matthias Lott²

¹RWTH Aachen University, Chair of Communication Networks, Aachen, German

²Siemens AG, Communications, Munich, Germany

¹{mst|dbn}@comnets.rwth-aachen.de, ²matthias.lott@siemens.com

Abstract – Future wireless communication systems will feature by a high degree of interoperability for which system integration is commonly regarded as an important aspect. To allow for smooth network migration, Vertical Handover (VHO) thereby is one of the key enabling technologies. Within this paper, VHO simulations are presented and analytically verified to demonstrate maintenance of services in a patchy WLAN environment. To allow for optimized VHO triggering, an intelligent concept referred to as Hybrid Information System is presented. Anyway, prior to taking sophisticated handover decisions, knowledge on alternatively available systems needs to be present. This entails the initial detection of complementary systems, which directs the system integration aspect to the problem of coverage detection. The present paper copes with this problem by proposing a new algorithm, referred to as Centre of Gravity. The algorithm evaluates densities of location related measurement reports whereby special attention is put on inherent positioning errors.

Keywords: System Integration, Vertical Handover, Coverage Detection, Centre of Gravity, Hybrid Information System

1. Introduction

Next generation wireless systems are broadly expected to feature by incorporative aspects. The reasons for this are manifold:

First, the perception that dedicated systems are more suitable to provide specific services to the user will result in complementary system design. Even today, different systems for ultra short-range, short-distance and wide area communication exist. This leads to specific deployments of Personal Body Networks (PAN), Wireless Local Area Networks (WLAN) and Cellular Networks.

Second, cooperation of systems in the same or adjacent spectrum will further increase. Due to spectrum scarceness, deregulation efforts for increased market competition and political reasons, the number of systems operating in direct impact sphere of each other will further increase. To allow for proper incorporation “live and let live” doctrines are necessary. Research in this field includes listen before talk approaches, frequency sharing rules for dynamic and static sharing and game theoretical approaches [1].

Third, the migration from current 2.5/3G systems to systems beyond 3G will proceed stepwise. This means, that future systems need to entail a certain degree of backward compatibility. Coexistence with previous generations thus is an existential requirement.

1.1. Contribution and Outline

The present paper copes with these challenges by addressing enhanced system integration aspects. Specifically, the VHO as a means to allow for (seamless) network migration is of particular interest. A new concept for VHO control, the Hybrid Information System (HIS), is presented. Features of the HIS are concatenation of system specific measurements with location information. The resulting *link state maps* serve as basis for inter-system VHO decision control, for which two approaches are considered: In the first case, HIS inherent data bases dispose of very accurate up-to-date (short-term) system information based on which VHO control is executed. In the second case no active entries are available, which means that only old (long-term) reports may be used for handover control. Further on, erroneous positioning is considered. To provide reliable coverage detection a new algorithm, called *Centre of Gravity*, is introduced.

The remainder of this paper is organized as follows: Section 2 provides an overview on system integration efforts with special focus on VHO. Section 3 presents an application scenario that is used for HIS controlled VHO investigations in Section 4. Since HIS relies on location specific measurement reports, the problem of erroneous positioning plays an important role. The Centre of Gravity algorithm that copes with this problem is presented in Section 5 and evaluated in Section 6. Section 7 finally concludes this paper with a summary.

2. System Integration

Following the evolution from 2G, over 3G and beyond, one will realize that the immanent drivers for this development are the user’s basic needs for mobility and communication. Accordingly, different mobile and wireless communication systems have been designed – and will be designed. At the same time, services as known from fixed networks are expected to be adapted to wireless media as well.

However, it is not very likely that one single system will ever be able to deal with all demands of modern communication: Quality of Service, security, maintainability, operation and deployment costs, spectrum scarceness, convenience, politics and health are only a few aspects that are hard, if not impossible to be optimized in parallel due to their partly contradictory objectives. Instead, the cooperation and bonding of dedicated technologies, each of which optimized for a dedicated field, seems to be an interesting alternative.

2.1. Related work

For the mentioned reasons, system integration is of fundamental interest. Projects in the 5th European Framework Programme addressed different kinds of interworking. General heterogeneous access was scope of DRIVE, TRUST and MOBIVAS. WINE GLASS focused on UMTS/WLAN integration whereas SUITED further considered GPRS and Satellite networks. The joint usage of heterogeneous systems with ad hoc networks finally was addressed in MIND and the Chinese FuTURE program. All the above mentioned activities have been enclosingly summarized and evaluated by the Network of Excellence ANWIRE [2].

Meanwhile, the 6th FP is on its way and system integration has become a central objective. New air interfaces as defined in WINNER [3] will entail inter-system properties, e.g. measurement support, straight from the beginning and E2R [4] pushes the property of reconfiguration to achieve support of different networks. Ambient Networks [5] finally follows the objective of a complete, coherent wireless network solution.

All the above projects basically aim on achieving the Always Best Connected [6] dogma. A key enabling technology thereby is the (seamless) incorporation of different networks, especially during ongoing communication processes, referred to as *Vertical Handover* (VHO).

2.2. Necessity for Vertical Handover

According to the supported coverage of complementary systems, one distinguishes between *upward* and *downward* VHO. Upward VHO denotes the switching from a system with smaller cell sizes and usually higher bandwidth to a wireless overlay with larger cell sizes and usually lower bandwidth per unit area. Downward VHO is the handover in the other direction, respectively. Figure 2 depicts both HO types.

In contrast to Horizontal HandOver (HHO), which denotes the intra-system handover between adjacent cells of the same system, VHO introduces further degrees of choice. As such, it might be possible that a decision unit triggers VHO execution due to QoS aspects, though the actual link quality is excellent. If namely another, vertical system with a multiple of offered data rate is available the decision space is no longer solely restricted to link parameters.

The main application scenario, to be investigated in many specifications though, will be the connection of a Mobile Terminal (MT) to a system A (high coverage, moderate bit rate) with some intermediate handovers to another, vertical system B (low coverage, high bit rates) and probably back to System A again. The described case corresponds to a transition of a hotspot by a mobile device, see Figure 1. Accordingly, VHO is one possible means to allow for (seamless) service continuity across network boundaries. Anyway, prior to taking sophisticated handover decisions, knowledge on alternatively available systems needs to be present. This entails the initial *detection* of complementary systems. Especially, if mobility is involved, the accessible infrastructure changes quickly.

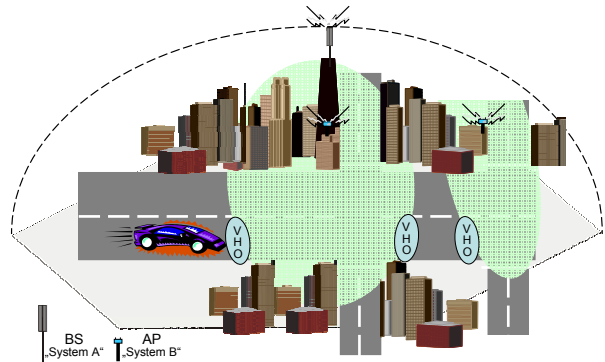


Figure 1: VHO Scenario with overlaying systems

This directs the system integration aspect to the problem of coverage detection that needs to be solved prior to further actions. Coverage detection is conventionally realized by means of self-conducted scanning. However, it was shown in [7] that this may harm both, own but also other transmissions. Alternatively, one could imagine that the coverage area of the potential system is known due to measurements taken previously by other terminals. A concept that exploits foreign party based measurements, administers them in (long-term) data bases and makes them available to other stations is presented in the next section.

2.3. Hybrid Information System

Within the previous section it was pointed out that self-conducted scanning is not a preferable means to gather system information. Another approach is to employ foreign party based measurement reports (MRs) as initially proposed for the HIS in [8].

The basic idea behind the HIS approach is illustrated in Figure 2. Each system reports about the current state, i.e. the link condition including, e.g., interference distribution. The resulting MR is associated with the position of the reporting mobile, see (1), for which self- or remote localization may be applied. The data is stored in a data base (2) such that mobiles of another system willing to change may request this information, cf. (3,4,5), to decide for VHO execution, (6). Alternatively, the decision may be taken by the HIS and signalled to the MT.

The HIS is both, an intelligent concept facilitating inter-system cooperation and a means to allow for context transfer between different systems. Subject of the HIS is to perform accurate detection of complementary systems and to initiate optimal VHO execution by respective triggering. In all cases, the HIS approach offers a great economic potential since participating devices can minimize or even avoid self-driven scanning.

2.4. Trigger and Trigger Origins

In general, triggers are pieces of information that indicate changes of setup or surrounding conditions. A commonly used definition within IETF says that “An L2 trigger is an abstraction of a notification from L2 (potentially including parameter information) that a certain event has happened or is about to happen” [9]. While the actual triggers from L2 to L3 are supposed to be of generic nature, inputs (=trigger origins) to L2

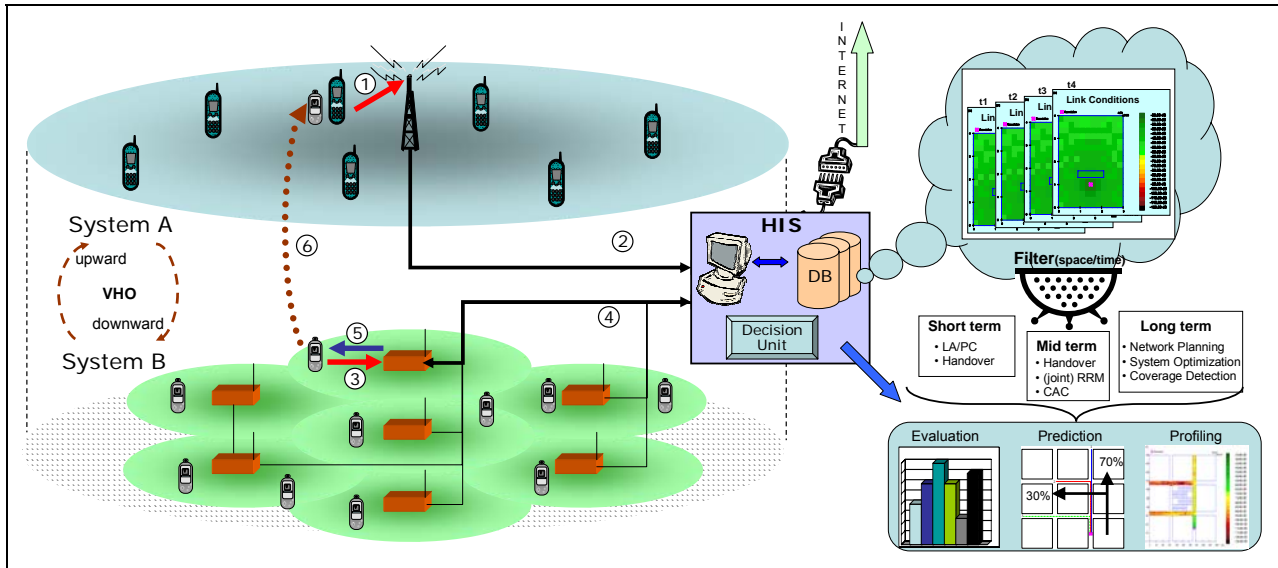


Figure 2: Hybrid Information System with location specific measurement reports and data bases

algorithms that decide on firing a trigger to higher layers are manifold – and system dependent. The reason for which a trigger finally is fired may be a direct response to an incoming L1 measurement, e.g. signal strength, or L2 based evaluation, e.g. resulting Bit Error Rate (BER) or number of counted negative acknowledgements (NACKs). A similar trigger classification was also used in MIND [10], where physical-based L2 triggers and algorithm-based L2 triggers were distinguished.

The HIS as described earlier entails a decision unit that takes into account trigger origins as input and produces handover recommendations (=triggers) as output. The advantage is, that the HIS is not restricted to local and system specific trigger origins. Besides incorporation of a multiple number of systems, HIS supports load balancing and joint radio resource management. Further, due to its backbone connection, see Figure 2, specific user preferences may be requested from e.g. the home network provider and incorporated in any decision process. Thus, HIS supports intelligent inter-system-control by combined evaluation of various trigger origins.

3. Application Example for VHO Support

Audio and video streaming services commonly require higher bandwidth than telephony services. Since UMTS is not able to carry many high bit rate streaming services [11], WLANs like 802.11 are candidate systems for future support of UMTS in hotspot areas. However, due to the inherent low coverage of WLANs, solutions for end-to-end service continuity while exploiting a combination of UMTS and WLAN need to be found.

Using buffering techniques, streaming services can be supported for a certain amount of time with reduced bandwidth available. Patchy 802.11 coverage areas may be bridged by using UMTS to support services with reduced bandwidth. Figure 3, which is a more formal presentation of the scenario in Figure 1, shows a Manhattan scenario with two access points (APs) placed at road crossings. The corresponding hotspots do not

overlap, thus, MTs moving along the street will face an interruption of WLAN connectivity and continuous transmission is only possible to the overlaid UMTS network (not shown in Figure 3). It is assumed that mobile users leaving AP1 coverage were able to completely fill their *reception* buffer. For initial investigations, the buffer size was chosen to cache 2000 packets each of which carrying 160 Byte data. When moving towards AP2 the service may be carried on simply by consuming buffered packets, indicated by d_{Buffer} . Thus, d_{Buffer} is the distance a certain service can be further maintained *without* switching to UMTS right after leaving WLAN.

However, by performing VHO to the UMTS network the service may be supported even longer, though UMTS itself is not able to carry the whole offered load required by the service. The *additional* distance is indicated by d_{UMTS} . The total distance the terminal may move without the service breaking down is calculated by equation 1. Table 1 shows exemplary distances for selected services. The data rate that is received within UMTS is assumed to be $\mu_{\text{UMTS}} = 64$ kbit/s. The mobile terminal's velocity was set to 30km/h. It can be seen that there is a significant distance (for special services only) that mobile users may travel without reaching another WLAN hotspot. The previous investigation helps in deriving deployment rules for installation of WLAN technology. Assuming an overlay UMTS network, one can such derive upper distance limits between adjacent APs superseding the necessity for full coverage under the assumption of average velocities of MTs.

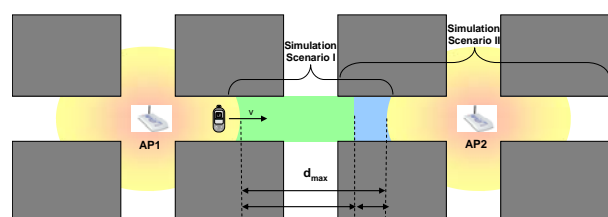


Figure 3: VHO simulation scenario

$$d_{\max} = d_{\text{Buffer}} + d_{\text{UMTS}} = \frac{L_Q}{\lambda_{\text{Service}} - \mu_{\text{UMTS}}} |\vec{v}| \quad (1)$$

Table 1: Distance bridged by buffering & UMTS

Service	Bit rate λ_{Service}	Distance d_{\max}
MP3 Stream (avg.)	128 kbit/s	333 m
MP3 Stream (good)	256 kbit/s	111 m
Video Stream	2 Mbit/s	11 m

On the other hand, if the distance of two already existing neighbouring APs and MT velocity are known, one can estimate the best possible service (in terms of throughput) that still can be supported.

4. Vertical Handover Control by HIS

To evaluate VHO performance, a simulation environment was created that allows for investigation of switching between UMTS and IEEE 802.11. VHO for multiple mobile stations is controlled by the HIS. To simulate mobile stations equipped with both, UMTS and IEEE 802.11, two existing protocol simulators were coupled¹. Figure 4 depicts the resulting simulator architecture. Proper control of traffic generators and context transfers between both simulators allow for VHO investigations. An evaluation instance encompassing both simulators allows for throughput, queue length and delay analysis.

The following section presents VHO simulation results for Simulation Scenario I, see Figure 3 and Figure 5, under entire control of the HIS. The scene starts at $T_{\text{up}} = 0$ s, right after VHO execution from WLAN (AP1) to UMTS (Node B). While the *reception* buffer at the MT's side is assumed to be completely filled, cp. Section 3, the *transmission* buffer at the Node B's side is assumed to be completely empty. Such, after the mobile has left WLAN coverage, transmission takes place via UMTS to the NodeB. The question of coverage detection and VHO triggering was solved by the HIS. Monitoring the current MT's position and being aware of coverage borders due to well established long-term evaluation of previous probes, no further effects due to blurred borders are considered for Scenario I. Depending on the MT's

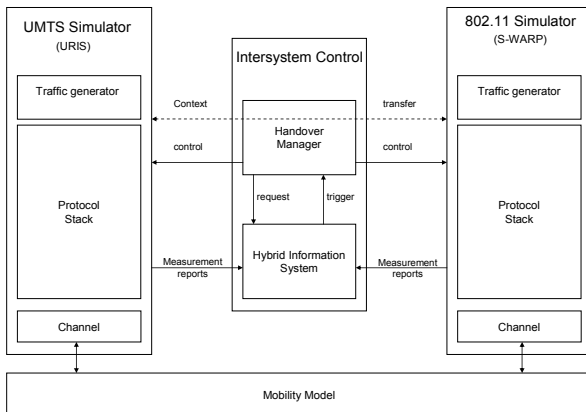


Figure 4: Overall Simulation Concept and Coupling

¹ For a more detailed description of our UMTS simulation environment URIS and the WLAN simulation environment S-WARP, please refer to [1][12].

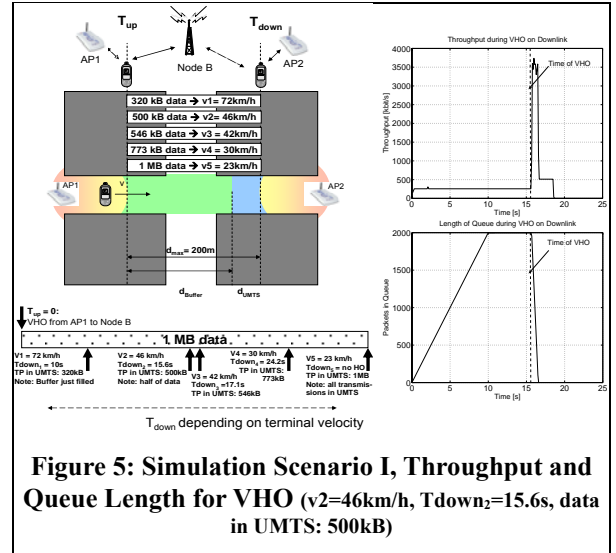


Figure 5: Simulation Scenario I, Throughput and Queue Length for VHO ($v_2=46\text{km/h}$, $T_{\text{down}2}=15.6\text{s}$, data in UMTS: 500kB)

velocity (v_1-v_5), it takes a different amount of time until the coverage area of AP2 is reached. In contrast to Section 3 where the aim was to derive a maximum distance d_{\max} between two APs for which a running service can be maintained, the following investigations focus on packet delay adjusting a fixed transition zone value of $d_{\max} = 200$ m. Since the load bit rate is of constant nature due to the assumed streaming service, different amounts of data are to be transferred within UMTS during the transition from AP1 to AP2. The corresponding data volumes as transferred within UMTS for different velocities are depicted in Figure 5. The target volume for which a final evaluation is performed amounts 1 MB. If a VHO from UMTS to WLAN (time: $T_{\text{down}1-5}$) is triggered before 1 MB of data was conveyed, the remaining amount of data is transferred across the 802.11 link (AP2).

Since the terminal is assumed to start using a service (here parallel download of 2 MP3 streams) the offered service load is set to 512 kbit/s. When leaving coverage area of AP1 ($t = T_{\text{up}} = 0 \rightarrow$ start of evaluation) a VHO to UMTS is performed. However, since UMTS is not able to carry many high bit rate streaming services, the respective UMTS radio link was limited to carry 256 kbit/s in average. Accordingly, the number of packets queued in the system is expected to rise, see Figure 5. When reaching coverage of AP2, a downward VHO is triggered. Due to its high bandwidth, 802.11 can carry the entire offered load of 512 kbit/s. In addition, spare capacity is used to transfer packets within the queue.

Figure 5 shows the throughput and queue length evaluation for the measured downlink for $v_2 = 46\text{km/h}$. The VHO is triggered at $T_{\text{down}2} = 15.6$ s, corresponding to 500 kB of data that have been transferred in UMTS. Hence, half of the fixed amount of data (1 MB) is transferred within UMTS and the other half is transferred hereafter within 802.11. It can be seen that VHO is triggered at about 15.6 s after simulation start. Prior, the Node B is able to transmit the offered load at a rate of 256 kbit/s. Since UMTS is not able to carry the entire offered load, the remaining packets are queued. Packets are put to the queue until a maximum queue size of 2000 packets is reached. Further arriving packets are dropped. When the handover is triggered the queue

is transferred to the WLAN system and transmission continues within 802.11. The actual queue transfer is not scope of this paper. One solution is to apply backbone context transfer as described in [2]. After VHO, the MT's link to the AP is able to carry much more traffic and transmits at the capacity limit of approx. 3.5 Mbit/s until the queue has been emptied. Hereafter, transmission continues until the target amount of data (1 MB) has been transferred.

Figure 6 shows the queue length of all simulations (v_1 - v_5) and the corresponding packet delay Cumulative Distribution Functions (CDF). The case described before (v_2) is included as well. It can be seen from the queue length figure that VHO is triggered at different times ($T_{down1} - T_{down5}$). The characteristic of all queue length plots is very similar: The rising edge of the queue plots is identical being directly related to the difference between offered load and carried traffic of UMTS. A special case is when the VHO is triggered after 320 kB have been transmitted (v_1). No packets are dropped in that case. The curve parameter is the amount of data transferred within UMTS before VHO is triggered. In the case that all packets are transmitted across the UMTS connection (v_5), the queue is filled and is never emptied since no VHO is triggered. As queue length increases the delay increases, too.

The waiting time τ_w for a packet transmitted at time T can be analytically verified by applying models from queuing theory. The investigated case corresponds to a D/G/1-FCFS model using a two-point distribution for the service rate μ . To derive a delay value τ_w , equation 2 needs to be solved. L_Q hereby denotes the queue length given by the scenario parameters λ (arrival rate of packets = load generated by streaming service), μ_{UMTS} and μ_{WLAN} (service rates by UMTS and WLAN), T_{down} (time of VHO from UMTS to WLAN). T_{Qfull} (time when queue reaches L_{Qmax}) and T_{Qempty} (time when the queue is processed after VHO) are a function of the maximum queue size L_{Qmax} and the arrival and service rates.

$$\int_{T-\tau_w}^T \mu(t)dt = L_Q(T - \tau_w) \times P_s \quad (2)$$

P_s represents the chosen packet size. Assuming no initial queue at simulation start ($L_Q(0) = 0$), the right part of equation (2) is given by:

$$L_Q(t) \times P_s = \begin{cases} (\lambda - \mu_{UMTS}) \cdot t & t < T_{Qfull} \\ L_{Qmax} \times P_s & T_{Qfull} \leq t < T_{VHOdown} \\ L_{Qmax} \times P_s - (\mu_{WLAN} - \lambda)(t - T_{VHO}) & T_{VHOdown} \leq t < T_{Qempty} \\ 0 & t \geq T_{Qempty} \end{cases} \quad \begin{matrix} \text{before} \\ \text{HO} \\ \text{after} \\ \text{HO} \end{matrix} \quad (3)$$

Equation 2 cannot be solved for all time instances easily. Nevertheless significant points in the delay distribution can be verified. The maximum delay in Figure 6 is $\tau_{wmax} = 10s$. These are packets occupying the last slot in the queue and are transferred solely within UMTS prior to VHO to WLAN. Therefore $L_Q(t) = L_{Qmax}$ and $\mu(t) = \mu_{UMTS} = const$, such that (2) becomes:

$$\tau_{wmax} = \frac{L_{Qmax} \times P_s}{\mu_{UMTS}} = \frac{2000 \cdot 160 \frac{\text{byte}}{\text{Packet}}}{256 \frac{\text{kbit}}{s}} = 10s \quad (4)$$

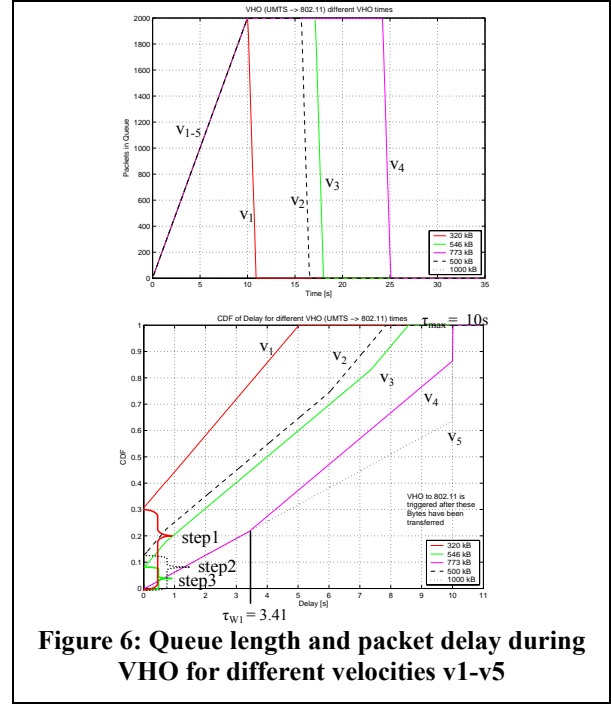


Figure 6: Queue length and packet delay during VHO for different velocities v_1 - v_5

In case that VHO is triggered after 773kB ($v_4 = 30\text{km/h}$, $T_{down4} = 24.2s$) have been transmitted within UMTS, a remaining data volume of 227 kB is transferred within WLAN. Keeping in mind that the assumed queue consists of 2000 packets, each of which carrying 160 bytes, this results in 320 kB that are transferred during the handover from UMTS to WLAN for subsequent transmission. Looking at Figure 6, one can see that the queue is entirely filled when the VHO is triggered. This means, that none of the packets that arrive after VHO execution is of interest for the delay evaluation (remember: simulation stops after an E2E transfer of 1 MB). Therefore, the last packet that is evaluated is transmitted after:

$$T = T_{VHO} + \frac{227 \text{ kByte}}{\mu_{WLAN}} = T_{VHO} + 0.52 s \quad (5)$$

All packets that are conveyed by WLAN originate from UMTS, therefore $T - \tau_w \leq T_{VHO}$. Solving (2) for these boundary conditions gives the value for τ_w , (equ. 6). Evaluation for the last packet transmitted after VHO gives $\tau_{w1} = 3.41 s$, see Figure 6.

$$\tau_w = \frac{L_{Qmax}}{\mu_{UMTS}} - \left(\frac{\mu_{WLAN}}{\mu_{UMTS}} - 1 \right) (T - T_{VHO}) \quad (6)$$

This explains the increased probability of packets with a delay between τ_{w1} and τ_{wmax} for the packet delay curve when VHO is triggered after 773 kB have been transferred.

In a similar approach, other significant values may be verified. Early VHO triggering due to increased terminal velocity ($v_1 > v_2 > \dots > v_5$) results in more and more packets being directly transferred within WLAN without previous waiting. Transmission delay within WLAN is very low, which yields to a step (step1 > step2 > step3) in the beginning of the packet delay CDF. Further changes of the gradient of the delay CDF for 500 kB and 546 kB cannot be easily verified with the above equations since waiting within both, UMTS as well as WLAN is included.

5. Triggering with noisy Reports

So far, HIS based VHO handover triggering was assumed knowledge of *exact* WLAN cell borders. However, as indicated in Figure 1, the VHO zone is more like a blurred area rather than a strict line. An important reason for this is that, besides radio inherent interference and fading, MRs based on which coverage detection is performed, are not exact, but are afflicted with positioning errors. Such, VHO decision algorithms need to find a way to compensate fuzziness of the cell border. The following section copes with this problem by proposing a new method for determining the coverage area based on evaluation of (erroneous) measurement reports.

5.1. Measurement Reports for Coverage Analysis

Detection of WLAN coverage relies on respective measurements. For the here considered case, the exploitation of RPI histograms as specified in 802.11h [13] is appropriate. To compile an RPI Histogram report, the observing station performs measurements during well defined measurement durations. For the whole measurement duration, the measured RPI is classified in one of 8 levels according to Table 2. In the end, the fraction of time for each level is reported.

Figure 7 shows RPI levels as a function of distance assuming free space propagation. A transmitting AP thereby is assumed at position 0 m, while a receiving MT at position X would recognize the respective RPI level. A simple one slope propagation model with a pathloss coefficient of $\gamma = 2.4$ is applied [14]. Each PHY Mode requires a minimum sensitivity level for successful reception. The according thresholds are shown in Figure 7, too. The shown boundaries are best-case distances, significantly decreased with interference. As can be seen from Figure 7, MR which include measured RPI levels to the AP of at least RPI 2 indicate that transmission is just possible applying BPSK1/2. Due to the minimum sensitivity requirement as specified in Table 3, the coverage area is bounded by a sharp theoretical maximum distance. However, real cells feature by a more diffuse border taking into account fading effects and interference.

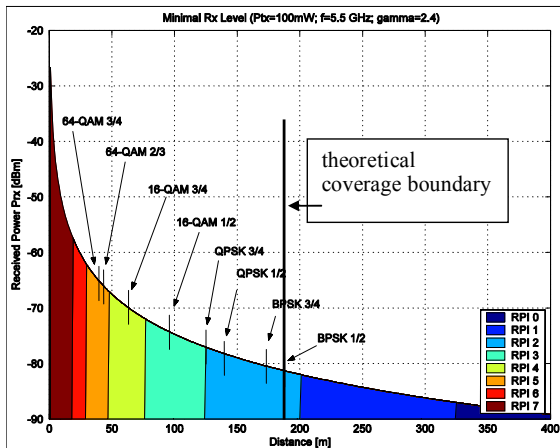


Figure 7: RPI levels for simple propagation model and sensitivity borders for PHY-modes

Table 2: RPI definitions due to 802.11h [13]

RPI Level	Power Observed at Antenna (dBm)
0	$[-\infty, -87]$
1	$[-87, -82]$
2	$[-82, -77]$
3	$[-77, -72]$
4	$[-72, -67]$
5	$[-67, -62]$
6	$[-62, -57]$
7	$[-57, +\infty]$

Table 3: Receiver Sensitivity [15]

Modulation	Minimum Sensitivity
BPSK $\frac{1}{2}$	-82 dBm
BPSK $\frac{3}{4}$	-81 dBm
QPSK $\frac{1}{2}$	-79 dBm
QPSK $\frac{3}{4}$	-77 dBm
16QAM $\frac{1}{2}$	-74 dBm
16QAM $\frac{3}{4}$	-70 dBm
64QAM $\frac{2}{3}$	-66 dBm
64QAM $\frac{3}{4}$	-65 dBm

A. Problem Statement

An algorithm for VHO triggering must be able to identify cell boundaries accurately. Erroneous localization introduces measurements that imply coverage at positions actually *not* within the cell. These measurements are shown in Figure 8, displayed as white dots outside the cell boundary. Obviously, these measurements in fact have been recorded *inside* the coverage area of the AP but due to erroneous localization the corresponding position was determined to be out of the coverage area. A new MT that approaches the coverage area of the corresponding AP will request whether MRs for its current position are available. If so, the corresponding MRs will be taken as basis for the VHO decision. Recommending a VHO based solely on these reports would result in a handover try after whose execution the terminal would not be able to attach to the sought cell. For this reason, the white dots are referred to as ‘misleading’ reports.

On the other hand, one can rely on the fact that MRs indicated to be within the cell boundary are always correct; see black dots in Figure 8. Thereby, ‘correct’ does not mean that localization may not entail the same fuzziness as for the misleading white dots. In fact, exactly the same fuzziness applies for these dots with the difference, that the position space representing the erroneous sojourning area is completely covered by the AP. The problem for a handover algorithm now is to distinguish between misleading and correct reports. Since the sole existence of a MR obviously is no warranty that the target area is really part of the coverage area, more sophisticated evaluation is to be applied.

B. Centre of Gravity Algorithm

In order to derive a clear decision whether coverage is given, a respective algorithm needs to evaluate particular MRs. Therefore, only local reports close to the cell border area should be considered. This is why a so called *Decision Area* (DA), see Figure 8, was introduced. To support the decision algorithm the *Centre of Gravity* (CoG) of all MRs within the DA is calculated. The distance d of the MT's position to the CoG is then compared to a threshold Δ_{VHO} to generate the VHO trigger. With a well populated long-term database most of the MRs will be within the actual coverage area of the cell. Such, a *high MR density* will result inside the really covered area, see Figure 8, while

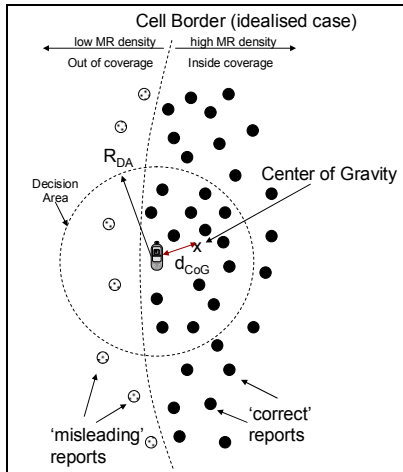


Figure 8: Distance to Centre of Gravity

a low MR density outside the really covered area will be measured. Approaching the coverage area of a cell, the distance between a MT's position and the calculated CoG is a characteristic curve (see Figure 9) of the degree of overlapping of the DA and the cell. Assuming the localization error distribution to be zero-mean the final distance between the centre of gravity and the MT's position will approach zero as soon as the complete DA is mapping the actually covered cell area. Figure 9 exemplarily depicts the distance to the CoG when an MT moves into the cell.

The distance firstly reported is the radius R_{DA} of the DA. Early MRs taken into account will be *misleading* reports, see (1) in Figure 9. Approaching the cell border will decrease the distance until a local minimum is reached, (2). Since there are much more MRs within the cell boundaries than there are *misleading* ones outside the cell border, the resulting distance d_{CoG} will increase again on further entering the cell, see (3). When the terminal approaches the actual cell border the distance will approach $R_{DA}/2$. If the mobile has moved into the cell, far enough that the whole DA is within the coverage area the distance will approach zero (4). By defining a minimal distance d_{min} , which needs to be reached and which needs to be below the local minimum introduced by the *misleading* measurements, a handover decision can be generated. The corresponding minimal distance d_{min} is also referred to as VHO trigger threshold Λ_{VHO} .

It should be mentioned that the algorithm's output actually is a distance vector. This vector \vec{d} points from the mobile terminal's position towards the CoG of all MRs within the DA. The distance vector \vec{d} has a tendency to point into the direction of higher MR area penetration. The angle between the velocity vector \vec{v} and the distance vector \vec{d} may be used to adjust the decision boundary d_{min} . MTs moving perpendicularly towards the cell border may have a higher d_{min} as mobile MTs moving tangential to a cell border. These MTs may even need very low thresholds to avoid repetitive ping-pong VHOs due to false handover triggers. As a rule of thumb d_{min} should be chosen a little below half of the DA's radius for perpendicular movement.

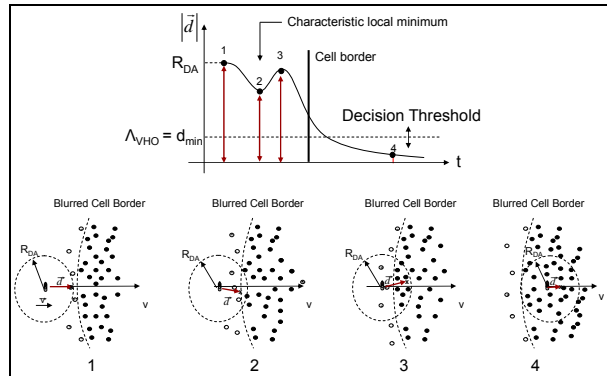


Figure 9: Centre of Gravity Algorithm: Identification of Handover Threshold

6. Simulation Results

The following section presents simulation results for the CoG algorithm exploiting long-term measurements for Scenario II, see Figure 3. The AP is located at the scenario centre, surrounded by four buildings, each of which with a length of 50 m. The space between buildings was chosen to 25 meters. Link state maps will be presented showing the received RPI levels. It shall be noted that all figures, thus, are based on actual measurements as recorded by MTs.

Unlike simulation based pathloss maps, derived from ray-tracing techniques as presented e.g. in [16], the here presented results correspond to 'real' probes meaning pieces of information that are really transmitted via the air interface. This entails that similar link maps may easily be derived in live networks.

B. HIS inherent Link State and Coverage Map

As described before, MRs are submitted according to 802.11h as RPI histograms. Within extensive long-term simulation runs, respective MTs moving around in the scenario have been requested to provide RPI MRs on a regular basis. MRs are requested every 200 ms, instructing the mobile to perform RPI histogram measurements for a duration of 10 ms. All MR have been stored as RPI Level histograms to a database for later investigation.

Figure 10 visualizes the gathered measurements. The visualization presented in the figure uses the exact positions to create a map of all received MRs. In reality these information will not be available. The exact positions were used to further verify the correctness of the simulator and to use the generated map to evaluate the performance of the cell border detection algorithm. For each position on the map all MRs are evaluated by calculating the mean RPI level reported. This value is represented in Figure 10 by the colour. At positions for which no measurements are available, RPI Level 0 is assumed. The AP is located at $x = 500$ m and $y = 500$ m. It can be seen that the maximum range that may be covered by the AP is about 191 m away from the cell centre. Communication is not possible when the received power drops below -82 dBm, which is the minimal sensitivity level required for BPSK1/2. The map does not show any measurements with an RPI 1. This is because no communication can be supported at that RPI level (compare Figure 7, Table 3).

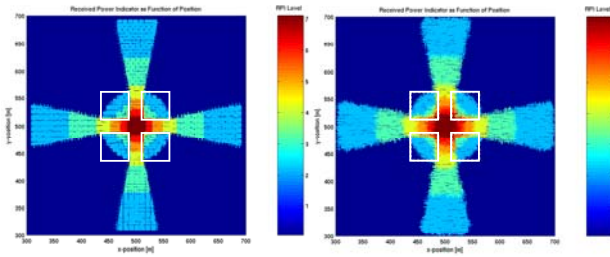


Figure 10: RPI level map with exact positioning

Figure 11: RPI level map using erroneous positions

Communication with the AP is not possible behind buildings. The wall attenuation is too strong such that the received power is below the minimal threshold of -82dBm . However, received power within buildings is still high enough to partially support communication. RPI values found within buildings are between RPI 3 and RPI 4. Figure 11 shows simulation results using erroneous position values. Such, real link state maps would reflect a picture similar to Figure 11 rather than Figure 10. Erroneous positions are modelled by Gaussian distributed errors with zero mean and variance of 100. In addition, the maximal error was limited to 10 m. It can be seen that imprecise positioning results in erroneous RPI zones and smooth transitions between received power indicators. Some MRs indicate incorrect values compared to the results shown in Figure 10. Within the buildings there are RPI Levels reported that belong to the area outside the buildings, some measurements imply that there is coverage behind buildings. Figure 12 gives a detailed view of the upper right quadrant of Figure 11. As stated, it can be seen that the density of (misleading) MRs outside cell borders (1) is lower than within the cell.

The aforementioned holds for transitions from one RPI level to the other, too (2). The effect of fuzzification is a direct consequence of the applied localization error distribution. Distributions with higher probabilities for large errors inherently feature by increased blurred cell borders and erroneous RPI transition zones.

6.1. Performance of Cell Border Detection

The following section evaluates the proposed *Centre of Gravity* algorithm for cell border detection. For this, the same long-term data that was used to generate the

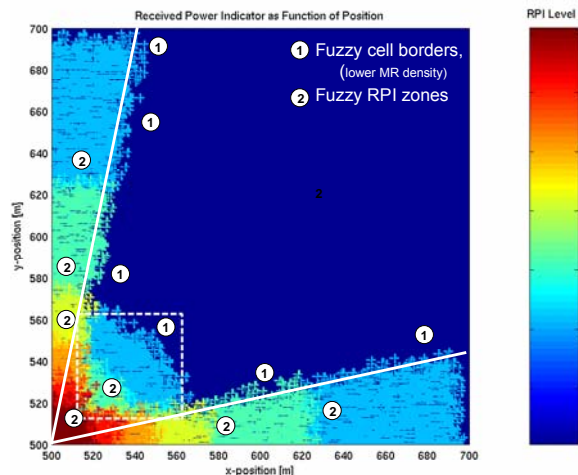


Figure 12: Details for map with erroneous positions

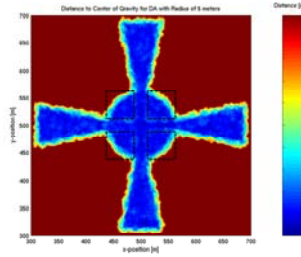


Figure 13: Distance to Centre of Gravity

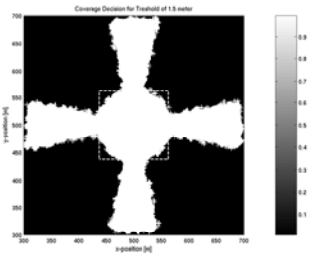


Figure 14: Coverage Detection

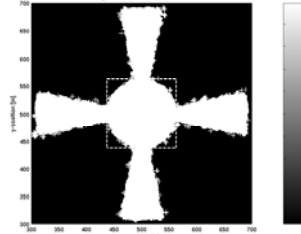


Figure 15: Coverage Detection (Thr. 0.9 m)

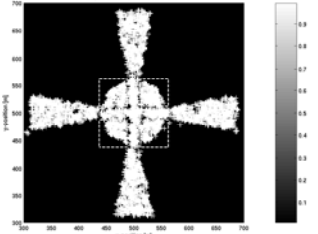


Figure 16: Coverage Detection (Thr. 0.2 m)

link state maps from Figure 11 (erroneous positions) is used for input to the algorithm. To decide whether a mobile is within the coverage area of the 802.11 cell, a DA is drawn around the mobile terminal's position. The radius of this area was set to $R_{DA} = 5\text{ m}$. To evaluate the precision and the performed error of the detection for the purpose of validation, the mobile's exact position is used as centre point for the DA area as reference. The algorithm was then applied to estimated positions associated with each MR. Figure 13 shows the distance from the mobile's position to the centre of gravity of all MRs within the MT's DA. This resembles the link state maps shown in the previous section. Outside the cell coverage area no measurements are found at all. At those positions the distance was set to the maximum distance of 5 m, which is the radius of the DA. It can be seen that the distance drops to zero when entering the cell. Figure 17 shows a cut of the distance map along the x-axis through the AP for the area around the cell border. Mobile terminals approaching the cell border initially observe a decrease of the distance to the centre of gravity. This is induced by misleading MRs placed outside the cell's coverage area, as explained in context of Figure 9. As soon as the DA enters the cell there is an increase of the distance since the measurement density is much higher within the cell. Only when entering the cell completely the distance drops below the local minimum introduced by MRs located outside the cell's coverage area. By such, the reported measurements as shown in Figure 17 entail exactly the same characteristic curve as presented in the centre of gravity concept in Figure 9.

A possible parameter for the CoG algorithm adjustment is the choice of the decision threshold d_{\min} . Figure 14 shows white areas where 802.11 is detected and black areas where no coverage was detected. The distance threshold was set to 1.5 m, which is still above the local minimum introduced by misleading reports. It can be seen that coverage is 'detected' at positions outside the cell's actual coverage area, e.g. there are some white areas behind buildings. Better results are

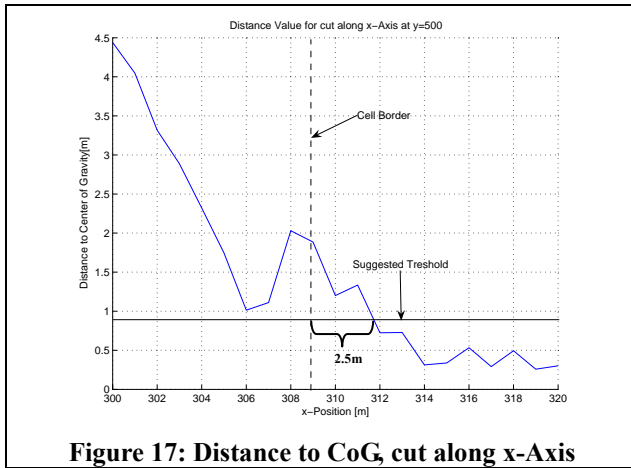


Figure 17: Distance to CoG, cut along x-Axis

achieved for a reduced threshold d_{\min} . Figure 15 shows the coverage detection map for a proposed threshold (thr.) of 0.9 m. This is more similar to the RPI level map gained from exact positioning shown in Figure 10, but still has some detection errors outside the cell coverage. A further reduction of the threshold leads to wrong detections made within the cell as indicated in Figure 16, where a d_{\min} value of 0.2 m was selected. It is to note that no further misleading detection outside the actual covered area is reported. However, this is obviously achieved at the cost of non-reliable detection inside the covered area. Thus, an acceptable compromise to ensure correct detection seems to be the chosen threshold $d_{\min} = 0.9$ m. This would allow for safe cell border detection while minimising the introduced loss to about 2.5 m, see Figure 17.

It has been shown, that the adjustable parameter d_{\min} represents a degree of freedom in the coverage detection process. Depending on the aspired accuracy and reliability of the cell coverage detection, this parameters may be chosen, while an upper limit d_{\min} according to the local minimum introduced by the CoG algorithm needs to be kept.

7. Summary

System integration is one important challenge with respect to future network development. One means to support network migration is the application of sophisticated VHO decisions.

Within this paper, properties of the Hybrid Information System (HIS) have been presented. The HIS has the role of an intelligent decision unit that stores measurement reports together with their location and takes over VHO control. Based on location-related measurement reports, the HIS calculates cell borders and signals a terminal to handover as soon as the target cell is reached. A patchy WLAN environment was chosen as exemplary scenario to demonstrate the maintenance of services. Due to buffering and VHO, respective services such can be continuously offered. In addition, deployment rules for installation of new APs can be derived and service support estimation for existing deployments becomes possible. The impact on E2E delay during VHO was analysed allowing to derive dimensioning rules for intermediate buffering; respectively handover triggering may be supported based on min/max delay requirements of services. All aforementioned simulations were based on the

assumption that sharp cell borders may be extracted by the HIS. Unfortunately, this is only an idealized assumption. Instead, blurred cell border zones according to fading effect and erroneous localization apply. The present paper copes with this problem by proposing a new method for coverage detection, referred to as *Centre of Gravity* (CoG) algorithm, based on density evaluation of (erroneous) measurement reports. The degree of overlapping between an adjustable decision area and the actual cell results in a characteristic curve with a local minimum. The decision threshold such can be defined whereby the upper margin must be below the local minimum. The selection of the threshold further can influence the detection reliability.

The CoG algorithm not only gives a scalar distance, but returns a vector towards the centre of gravity. This allows for estimation whether the mobile is moving towards the cell centre or whether it is just passing by. Accordingly, it may be applied in the context of ping-pong handover avoidance.

Further investigations of the CoG algorithm comprise dependency on the chosen shape and size of the decision area. In addition, dynamical aspects such as velocity dependent decision area shapes or dynamic adjustment of the threshold are of research interest.

REFERENCES

- [1] S. Mangold, "Analysis of IEEE 802.11e and Application of Game Models for Support of Quality-of-Service on Coexisting Wireless Networks", PhD Thesis, Chair of Communication Networks, ISBN 3-86073-985-9, June 2003
- [2] IST-2001-38835 ANWIRE, D1.5.1, "Integrated System and Service Architecture", June 2003
- [3] IST Project Winner (IST-2002-507581), <https://www.ist-winner.org/>
- [4] IST Project End-to-End Reconfigurability E2R (IST-2003-507995), <http://e2r.motlabs.com>
- [5] IST Project Ambient Networks (IST-2002-507134), <http://www.ambient-networks.org>
- [6] M. O'Droma et al., "ABC Enabled 4G Wireless World", 12th IST Summit on Mobile and Wireless Commun., Aveiro, Portugal, June 2003, pp. 710-16
- [7] Schinnenburg et al, "Enhanced Measurement Procedures for VHO in Heterogeneous Wireless Systems", 14th PIMRC, Sep. 2003, pp 166-171, Beijing, China
- [8] Siebert et al, "Hybrid Information System", VTC2004-Spring, Milan, Italy, May 17-19, 2004
- [9] IETF Internet Draft "Supporting Optimized Handover for IP Mobility - Requirements for Underlying Systems", June 2002, draft-manyfolks-l2-mobilereq-02.txt
- [10] IST-2002-28584 MIND, Deliverable D3.1, "Functional Specification of the Service Specific Convergence Sub-layer for IP and Analysis of new Functionality to support 'beyond 3G' System Aspects", May 2002.
- [11] B. Walke, M.P. Althoff, P. Seidenberg, UMTS – Ein Kurs, J. Schlembach Fachverlag, ISBN 3-935340-15-X, 2002
- [12] S. Heier, "Leistungsbewertung der UMTS Funkschnittstelle", PhD Thesis, Chair of Communication Networks, ISBN 3-86130-167-9, 2003
- [13] IEEE 802.11h, Wireless Medium Access Control (MAC) and physical layer (PHY) specifications: Spectrum and Transmit Power Management extensions in the 5GHz band in Europe, Draft Supplement to IEEE Std 802/11, 1999
- [14] B. Walke, "Mobile Radio Networks: Networking, Protocols and Traffic Performance", 2nd Edition, Wiley, 2001
- [15] IEEE 802.11a, High-Speed Physical Layer in the 5GHz Band. Technical Report, IEEE Computer Society. Draft Supplement to IEEE Std 802/11, 1999 Edition.80211.a
- [16] Seidel, Rappaport, "A ray tracing technique to predict path loss and delay spread inside buildings", Globecom 92, pp 649--653
- [17] IETF Internet Draft, "Problem Statement for Link-Layer Triggers work", (work in progress), draft-williams-l2-probstmt-00.txt, June 2002